Role of the β-Strand Insert in the Central Domain of the Fibrinogen γ-Module†

Sergei Yakovlev, Sergei Litvinovich, Dmitry Loukinov, and Leonid Medved*

Department of Biochemistry, The American Red Cross Holland Laboratory, Rockville, Maryland 20855

Received August 4, 2000; Revised Manuscript Received October 19, 2000

ABSTRACT: The crystal structure of the fibrinogen γ-module (residues γ143−411) [Yee, V. C., et al. (1997) *Structure 5*, 125−138] revealed an unusual feature. Namely, residues γ381−390 in the functionally important COOH-terminal region form a β-strand that is inserted into an antiparallel β-sheet of the central domain (γ192−286), while the rest (γ393−411) seems to be flexible. To clarify the structural and functional importance of this β-strand insert, we analyzed the folding status of the plasmin-derived fibrinogen fragment D_3 and several truncated variants of the γ-module expressed in *Escherichia coli*. It was found that D_3, in which most of the COOH-terminal domain of the γ-module (γ287−379) is removed proteolytically, retains a γ374−405 peptide that seems to be associated noncovalently with the bulk of the molecule via its β-strand insert region. A study of the denaturation−renaturation process of D_3 suggested that without this peptide its truncated γ-module remains folded but is destabilized. This was confirmed directly with the truncated recombinant variants of the γ-module, including residues γ148−392, γ148−373, and γ148−286. They all were folded, but those devoid of the β-strand insert were destabilized. The results indicate that although the β-strand insert contributes to the stabilization of the γ-module, it can be removed without destroying the compact structure of the latter. On the basis of this finding and some other observations, we propose a mechanism for the function-related conformational changes in the fibrin(ogen) γ-modules.

Fibrinogen (340 kDa) is a complex multifunctional plasma protein. It consists of two identical subunits, each of which is formed by three nonidentical polypeptide chains, Aα, Bβ, and γ (*1*). Both subunits and the six polypeptide chains are linked together by disulfide bonds and assemble to form at least 18 distinct domains grouped into four major structural regions, the central E, two identical terminal D, and two interacting αC domains (*2*−*4*). The E region is formed by the NH_2-terminal parts of all six chains; each αC domain is formed by the COOH-terminal portion of Aα chain, while each D region is formed by the remaining portion of the Aα chain and by the COOH-terminal portions of the Bβ and γ chains. These regions contain multiple binding sites that allow interactions of fibrin(ogen) with itself and with other proteins and cell types and its participation in a number of important physiological and pathological processes, including blood coagulation, fibrinolysis, inflammation, angiogenesis, wound healing, atherogenesis, and tumorigenesis. A comprehensive understanding of the role of fibrinogen and fibrin in these processes requires a detailed knowledge of its structure−function relationships.

Much of our knowledge about the interaction of fibrin(ogen) with itself and other molecules came from numerous studies with fibrin(ogen) fragments prepared by limited proteolysis or chemical cleavage. Among them are the E and D fragments derived from the central E and terminal D regions, respectively. The structure and functional properties of the plasmin-produced D_1 fragment (95 kDa) were well characterized. The NH_2-terminal portions of its Aα, Bβ, and γ chains form a triple-helical coiled coil domain (Figure 1A) that is involved in interaction with plasminogen and tPA (*5*, *6*) and with endothelial cells via their ICAM-1 receptor (*7*). The remaining homologous COOH-terminal portions of its β- and γ-chains, called the β- and γ-modules, respectively, form globular-like structures consisting of three independently folded domains, NH_2-terminal, central, and COOH-terminal (*4*, *8*, *9*). Both modules bind Ca^{2+} (*10*) and are functionally important. In particular, the γ-module (residues γ143−411) contains a major polymerization site, two cross-linking sites for factor XIIIa, and a tPA-binding site that are required for fibrin assembly and fibrinolysis (*11*−*14*). It interacts with platelets promoting their aggregation and interacts with leukocytes during the fibrin(ogen)-dependent inflammatory response (*15*, *16*). It also binds *Staphyllococus aureus* bacteria (*17*).

The crystal structure of the recombinant γ-module (*8*, *9*) revealed an unusual feature. Namely, in the central domain of this module (residues γ192−286), the middle β-strand of a five-stranded antiparallel β-sheet is formed by insertion of residues 381−390 from beyond the COOH-terminal domain (residues γ287−379); the remaining extreme COOH-terminal residues γ393−411 appear to be highly flexible (Figure 1B). The flexible part contains reactive Gln and Lys residues that are involved in γ−γ cross-linking between neighboring fibrin molecules and binds to platelets via their $\alpha_{IIb}\beta_3$ integrin receptor, and to bacteria. The γ381−390 β-strand insert represents a portion of the binding site for the leukocyte integrin receptor $\alpha_M\beta_2$ (Mac-1) (*18*). Interest-

† This work was supported by National Institutes of Health Grant HL-56051 (to L.M.).

* To whom correspondence should be addressed: The Holland Laboratory, American Red Cross, 15601 Crabbs Branch Way, Rockville, MD 20855. Telephone: (301) 738-0719. Fax: (301) 738-0794. E-mail: medvedl@usa.redcross.org.

10.1021/bi001836h CCC: $19.00 © 2000 American Chemical Society
Published on Web 11/23/2000

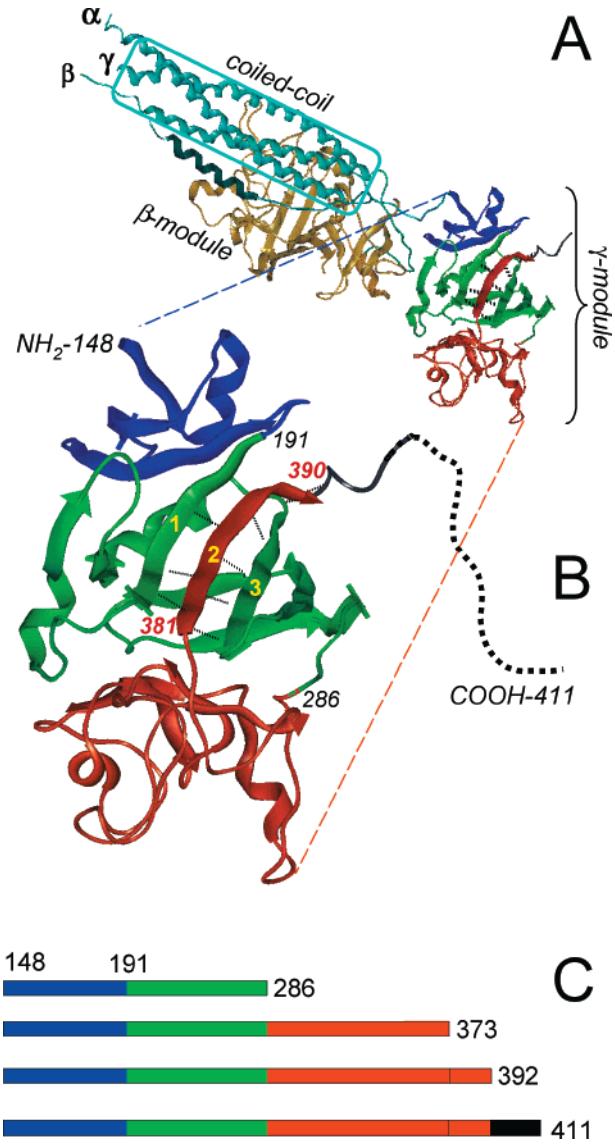

FIGURE 1: Spatial positioning of the γ381−390 β-strand insert in the three-dimensional structure of the fibrinogen γ-module and schematic representation of the truncated variants of the γ-module expressed for this study. Panel A represents the ribbon diagram of the D_1 fragment based upon its crystal structure (*9*). The coiled coil domain (boxed) and the β- and γ-module are shown. Panel B represents the enlarged ribbon diagram of the γ-module. The NH_2-terminal domain (residues 148−191) is in blue; the central domain (residues 192−286) is in green, and the COOH-terminal domain (residues 287−379) is in red. The β-strand insert (residues 381−390) is presented by red bent arrow 2, while the neighboring antiparallel β-strands of the central domain β-sheet are represented by green arrows 1 and 3. β-Strands 1 and 2 form the leukocyte-binding site (see the text). The extreme COOH-terminus (residues 392−411) whose position was not defined in the crystal structure is represented by a dotted line. The diagram was constructed using the computer program MOLE (Applied Thermodynamics, Hunt Valley, MD). Panel C represents schematically the γ-module and its truncated variants expressed for this study.

ingly, it was reported that this site is not fully exposed in fibrinogen (*19*) and that binding of fibrinogen to the platelet receptor results in the exposure of the RIBS-1 epitope (γ373−385) that includes part of the β-strand insert (*20*, *21*). These observations suggest that this unusually folded COOH-terminal portion of the γ-module may undergo function-related conformational changes upon interaction of fibrin(ogen) with its integrin receptors or upon conversion of fibrinogen to fibrin. The major goal of this study was to clarify the mechanism of such changes.

EXPERIMENTAL PROCEDURES

Proteins. Plasminogen-depleted human fibrinogen was purchased from Calbiochem. Plasmin was purchased from Sigma. The D_1 fragment was prepared from the plasmin digest of human fibrinogen as described previously (*22*). The D_3 fragment was obtained by further digestion of the D_1 fragment with plasmin in the presence of 10 mM EDTA as described in ref *23* with some modifications. Briefly, the D_1 fragment at 1−3 mg/mL was treated with plasmin for 14 h at 37 °C in TBS,[1] and the enzyme/fragment molar ratio was 1/50. To terminate the digestion, plasmin was inhibited by 0.1 mM PMSF and then removed from the incubation mixture by affinity chromatography on Lys-Sepharose. The D_3 fragment was isolated from the digest by size-exclusion chromatography on a Superdex 200 column using a Pharmacia FPLC system.

Peptides. Natural peptide γ374−405 was prepared from the D_3 fragment by high-performance liquid chromatography (HPLC) on a reverse-phase C18 Vydac column using a 0 to 50% gradient of acetonitrile with 0.1% trifluoroacetic acid. A synthetic peptide corresponding to the γ374−396 region was synthesized by SynPep (Dublin, CA) and additionally purified by HPLC on the same column.

Expression of Recombinant γ-Module Variants. A recombinant wild-type γ-module corresponding to residues 148−411 of the human fibrinogen γ-chain was produced in *Escherichia coli* using a pET-20b expression vector as described previously (*4*). This vector was used as a template to produce following COOH-terminally truncated variants of the γ-module, γ-t392 (residues 148−392), γ-t373 (residues 148−373),[2] and γ-t286 (residues 148−286) (Figure 1C). A cDNA encoding γ-t373 and γ-t286 variants was produced by polymerase chain reaction (PCR) using the following primers: 5′-TTTCCCTCTAGAAATAATTTTGTTTAACTTTAAG-3′ and 5′-TTTAAAAAGCTTTCATTTCCAAGTGGCCCAAATAATG-3′ for γ-t373 and 5′-TTTCCCTCTAGAAATAATTTTGTTTAACTTTAAG-3′ and 5′-TTTAAAAAGCTTTCAAGCATCCCCACCAGCGAAG-3′ for γ-t286. The PCR products were subcloned into the pET-20b expression vector (Novagen) using *Xba*I and *Hin*dIII restriction sites and then transformed into DH5α *E. coli* host cells (Life Technology). The cDNA fragments were sequenced to confirm that no error occurred during amplification. To produce γ-t392, a stop codon was introduced into the pET-20b plasmid containing cDNA encoding the wild-type γ-module at position 393 using the Transformer site-directed mutagenesis kit (Clontech). The plasmid was modified simultaneously with two mutagenic primers. One primer (5′-

[1] Abbreviations: TBS, 0.02 M Tris buffer (pH 7.4) with 0.15 M NaCl; PAGE, polyacrylamide gel electrophoresis; GdmCl, guanidinium chloride; γ-wt, recombinant wild-type γ-module (residues γ148−411); γ-t392, recombinant truncated γ-module (residues γ148−392); γ-t373, recombinant truncated γ-module (residues γ148−373); γ-t286, recombinant truncated γ-module (residues γ148−286); DSC, differential scanning calorimetry.

[2] We also expressed the truncated version, the γ-t379 fragment, that ends immediately before the β-strand insert. However, its monomeric form had low solubility, forcing us to express the γ-t373 fragment whose COOH-terminus ends immediately before the γ374−405 proteolytic fragment detected in D_3.

CCATTCAACAGACTCTAATCTAGAGAAGGACAGCA-ACACCAC-3′), complementary to the end of the γ148−392 fragment coding sequence, added a restriction site for *Xba*I downstream of the introduced stop codon to facilitate further analysis. Another primer (5′-GCTTGCGGCCG-CACTGGAGCACCACCACCACCAC-3′) eliminated the unique *Xho*I restriction site in the polylinker region of the target plasmid to facilitate screening. The screening for the desired mutation was performed by *Xba*I digestion of the plasmid DNA isolated from selected colonies of DH5α cells. The resultant clone was then sequenced to confirm the integrity of the coding sequence. The BL21/pLysS *E. coli* host cells were then transformed with the mutant plasmids, and the mutant variants of the γ-module were produced and refolded following the procedure previously described for the recombinant wild-type γ-module (*4*). The purity of the resulting mutants was verified by SDS−polyacrylamide gel electrophoresis and amino acid sequence analysis.

Amino Acid Sequence Analysis. NH_2-terminal sequence analysis was performed with a Hewlett-Packard model G 1000S sequenator. The NH_2-termini of the natural and recombinant fragments were determined by direct sequencing for 10 cycles. The natural peptides prepared from the D_3 fragment were sequenced for 35 cycles.

Protein Concentration Determination. Concentrations of the natural and recombinant fragments and the natural and synthetic peptides were determined spectrophotometrically using extinction coefficients ($E_{280,1\%}$) calculated from the amino acid composition with the equation $E_{280,1\%} = (5690W + 1280Y + 120S\text{-}S)/(0.1\ M)$, where *W*, *Y*, and S-S represent the number of Trp and Tyr residues and disulfide bonds, respectively, and *M* represents the molecular mass (*24*, *25*). Molecular masses of the fragments and peptides were calculated on the basis of their amino acid composition. The following molecular masses and $E_{280,1\%}$ values were obtained: γ-module, 29.7 kDa and 24.8; γ-t392, 27.9 kDa and 26.5; γ-t373, 25.4 kDa and 26.3; γ-t286, 15.8 kDa and 21.0; γ374−405 peptide, 3.7 kDa and 18.8; and γ374−396 peptide, 2.8 kDa and 24.8.

Fluorescence Study. Fluorescence spectra were recorded in an SLM 8000-C fluorometer. Fluorescence measurements of thermal- or chemical-induced unfolding were performed by monitoring either the intrinsic fluorescence intensity at 370 nm or the ratio of the intensity at 370 nm to that at 330 nm with excitation at 280 nm in the same fluorometer. The temperature was controlled with a circulating water bath programmed to raise the temperature at a rate of 1 °C/min. Protein concentrations were 0.02−0.03 mg/mL. GdmCl-induced unfolding was accomplished in the same instrument at 5 °C by continuous addition with a motorized syringe of a concentrated stock solution of the titrant (8 M GdmCl) at a rate of 20 μL/min to a stirred cuvette containing 0.85 mL of the protein solution (0.02−0.03 mg/mL) while monitoring the fluorescence ratio as described above. Both the fluorometer and the syringe driver were controlled by a computer which automatically corrected the fluorescence intensity for dilution assuming a linear dependence on protein concentration below 0.15 mg/mL.

Calorimetric Study. Differential scanning calorimetry (DSC) measurements were made with a DASM-4M calorimeter (*26*) in the temperature range of 5−130 °C at a scan rate of 1 °C/min, and protein concentrations varied from 1.0 to 1.5 mg/mL. The DSC curves were corrected for an instrumental baseline obtained by heating the solvent. Melting temperatures (T_m) and the enthalpies of denaturation were determined from the DSC curves using software provided by V. Filimonov (Institute of Protein Research, Pouschino, Russia). Deconvolution analysis was performed according to refs *26* and *27* using the same software.

RESULTS

Detection of the Noncovalently Associated Peptide in the Fibrinogen D_3 Fragment. It is well established that in the presence of EGTA plasmin converts the human fibrinogen D_1 fragment into a lower-molecular mass fragment D_3 (*28*). It is also commonly accepted that this conversion is accompanied by the removal from D_1 of the COOH-terminal region of its γ-module, including residues γ303−411 (*23*, *28*). At the same time, the crystal structure of this fragment (*8*, *9*) indicates that part of this region (residues 381−390) forms a β-strand insert in the central domain of the γ-module (Figure 1A,B). Since this insert may be an integral part of this domain, one can hypothesize that it could be retained in the native D_3 fragment. To test this hypothesis, we first analyzed the polypeptide chain composition of the D_3 fragment.

The D_3 fragment prepared as described in Experimental Procedures was additionally purified on a Superdex 75 column equilibrated with TBS to remove possible lower-molecular mass contaminants. NH_2-terminal sequence analysis of this fragment revealed four to six residues in each cycle. Computer-assisted comparison of the residues against the known sequence of D_3 allowed us to identify six sequences starting at AαD105, AαV111, BβD134, γS86, γM89, and γT374. The latter sequence starts very close to the β-strand insert, indicating that this insert is present in the D_3 fragment. This was further confirmed by reverse-phase HPLC and by size-exclusion chromatography.

Both HPLC and size-exclusion chromatography in denaturing conditions revealed two peaks, major and minor ones (Figure 2A,B). The material from these peaks was collected, analyzed by SDS−PAGE, and sequenced. The major peak in both cases contained material corresponding to the expected D_3 fragment, while the minor one contained a 4 kDa peptide corresponding to residues 374−405 of the γ-chain.[3] A shorter peptide, including residues γ374−396, was also detected in some preparations of the D_3 fragment. The $[D_3]$/[peptide] molar ratio determined by spectrophotometric measurement of the amount of material in each HPLC-obtained peak was 1/1. No minor peak was detected when size-exclusion chromatography was performed without GdmCl, suggesting that the peptide interacts with the bulk of the D_3 fragment. Thus, the results presented above indicate that the native D_3 fragment contains the noncovalently associated γ374−405 (or γ374−396) peptide that interacts with the fragment most probably via the γ381−390 β-strand insert.

Effect of the Removal of the β-Strand Insert on the Stability of the D_3 Fragment. To test the role of the γ381−390 β-strand insert in the structural integrity of the γ-module,

[3] A similar peptide (γ376−403) was found to be associated with bovine fibrinogen D_L fragment which is an analogue of the human fibrinogen D_3 fragment.

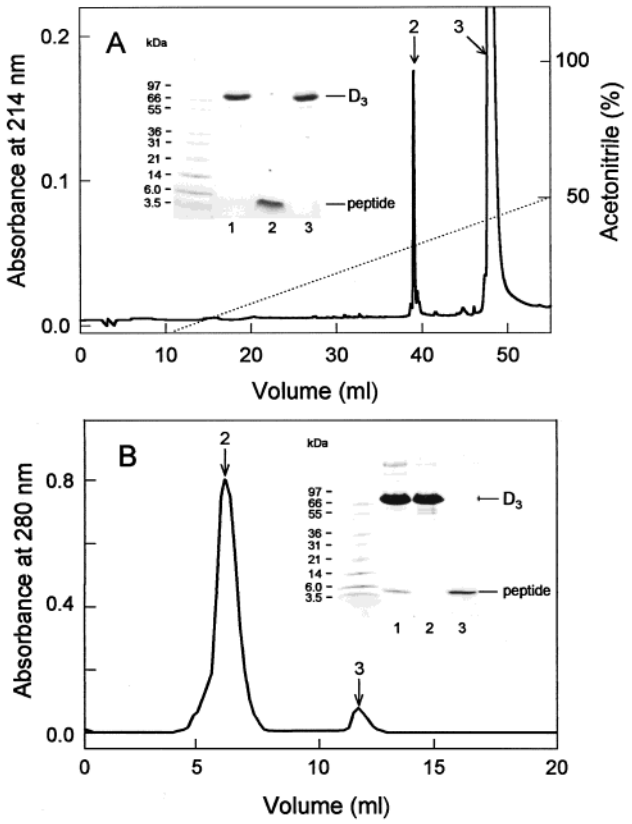

FIGURE 2: Detection of the noncovalently associated peptide in the fibrinogen D_3 fragment by HPLC (A) and size-exclusion chromatography (B). (A) HPLC profile of the D_3 fragment. The gradient of acetonitrile was applied as shown by the dotted line. (B) Size-exclusion chromatography of D_3 on a Superdex 75 column equilibrated with 20 mM Tris buffer (pH 8.0) containing 4 M GdmCl. The insets in both panels show SDS−PAGE analysis of the applied D_3 fragment (lanes 1) and the individual peaks indicated by arrows (lanes 2 and 3); the outer left lines in each panel contain molecular mass markers (Mark 12 Unstained Standard, Novex).

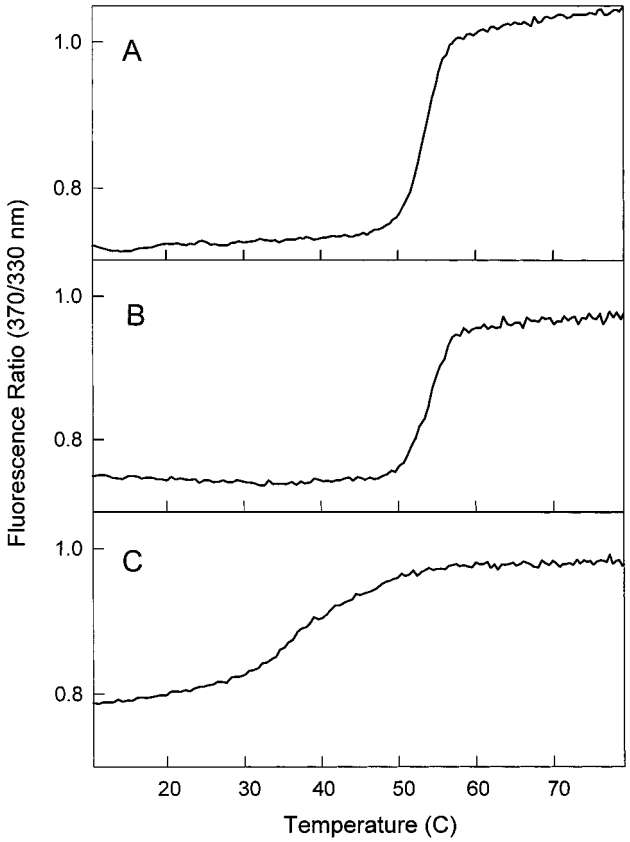

FIGURE 3: Fluorescence-detected thermal stability of the native and refolded species of the D_3 fragment. (A) Fluorescence-detected thermal denaturation of the native D_3 fragment. (B and C) Thermal denaturation of the D_3 fragment refolded in the presence and absence of the γ374−405 peptide, respectively. All experiments were performed in 100 mM Gly buffer (pH 8.6) with 0.5 mM Ca^{2+}.

we compared the thermal stability of the peptide-loaded and peptide-free D_3 fragment. The γ374−405 peptide was separated from the bulk of the molecule by size-exclusion chromatography on Superdex 75 as shown in Figure 2B. The peptide-free D_3 fragment was then refolded by slow dialysis from 8 M urea in the absence and presence of a 5-fold molar excess of this peptide. The refolding protocol was essentially the same as that described for the refolding of the γ-module (*4*). Both refolded species were passed through a Superdex 200 column, and the major fraction corresponding to the monomeric fragment was collected in both cases. Analysis by SDS−PAGE and HPLC of the D_3 fragment that was refolded in the presence of the peptide confirmed that the peptide was incorporated into the fragment in a 0.9/1 molar ratio.

The peptide-containing refolded D_3 fragment exhibited a fluorescence-detected unfolding transition similar to that in the native D_3 fragment (Figure 3A,B). Since this transition reflects unfolding of the central and COOH-terminal domains in the β- and γ-modules of the D fragment as reported previously (*4*), this result indicates that these domains in D_3 were refolded properly in the presence of the peptide. Similar results were obtained with a slightly shorter synthetic peptide, γ374−396 (not shown). The D_3 fragment that was refolded in the absence of the peptide also exhibited an unfolding transition; however, it started at a lower temperature and was much broader (Figure 3C). This result suggests that although the refolding of the γ-module in D_3 may occur without the peptide, the resulting structure is less stable. To test this suggestion, analysis of the individual γ-module and its truncated variants was required.

Characterization of the Recombinant Oligomeric γ-Module. While developing a refolding protocol for the recombinant γ-module, we noticed that although the protein remained soluble at pH 8.0, only 15−20% of it was found in monomeric form; the remaining material consisted mainly of soluble noncovalent oligomers that exhibited some fluorescence properties of a folded protein (*4*). Here we compared the folding status of the monomeric and oligomeric forms of the γ-module by differential scanning calorimetry (Figure 4). As reported previously (*4*), the heat absorption peak of the monomeric γ-module occurring at about 52 °C reflects the melting of its central and COOH-terminal domains. As expected, the monomer exhibited a heat absorption peak with a midpoint (T_m) at 50 °C that was easily fitted by two two-state transitions connected with the melting of these domains (Figure 4, curve 1). The oligomer also exhibited a heat absorption peak that was fitted by two two-state transitions (curve 2), indicating that its central and COOH-terminal domains are both folded into a compact structure. However, in the oligomer the peak occurred at lower temperatures than that in the monomer, indicating that both domains are destabilized. Remarkably, the shift in T_m (∼15 °C) brought it to a value similar to that in the peptide-

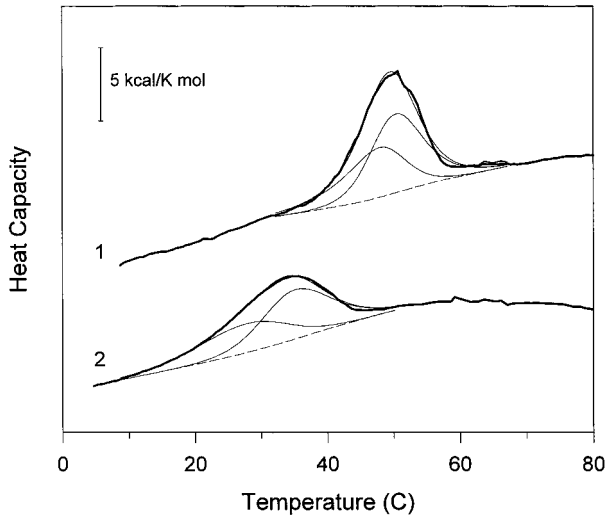

FIGURE 4: Differential scanning calorimetry curves of the monomeric (curve 1) and oligomeric (curve 2) forms of the recombinant γ-module. The thick solid lines represent the original curves obtained by the heating of the proteins in 100 mM Gly (pH 9.0) in the presence of 0.5 mM Ca^{2+}. The thin dashed lines indicate the manner in which the excess heat capacities were determined; the thin solid lines represent the component two-state transitions and the best fits obtained by deconvolution.

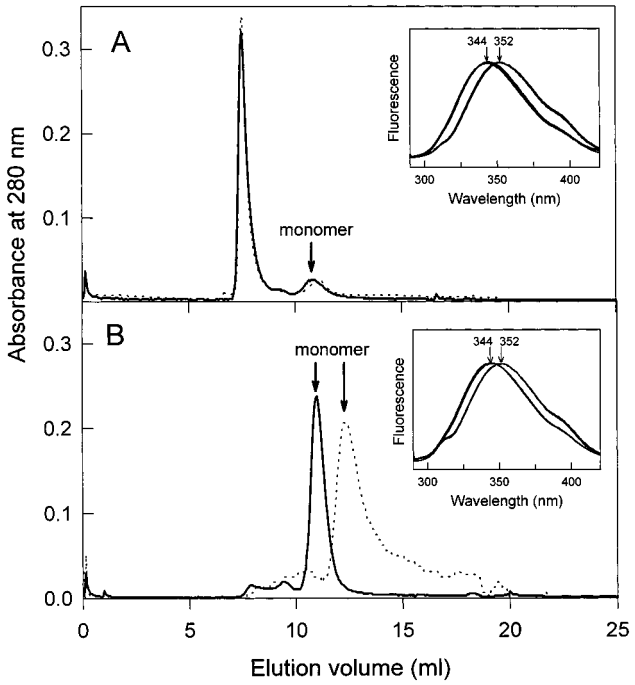

FIGURE 5: Size-exclusion chromatography and fluorescence analysis of the refolded recombinant γ-module and its truncated variants. Panel A represents elution profiles of the wild-type γ-module (dotted line) and its truncated variant γ-t392 (solid line) that essentially coincide. Panel B represents elution profiles of the γ-t373 (solid line) and γ-t286 (dotted line) truncated variants. The chromatography was performed on a Superdex 75 column equilibrated with TBS. Arrows in both panels indicate the peaks corresponding to the monomeric forms. The inset in panel A shows the fluorescence spectra of γ-wt and γ-t392 before and after refolding. The spectra of both species in 4 M GdmCl are superimposable with maxima at 352 nm. The spectra of refolded monomeric and oligomeric fractions of both γ-wt and γ-t392 are also superimposable with maxima at 344 nm. The inset in panel B shows the fluorescence spectra of γ-t373 and γ-t286 before (maxima at 352 nm) and after (maxima at 344 nm) refolding.

free D_3 fragment (Figure 3C). This suggests that in the oligomeric fraction of the γ-module, its γ381−390 β-strand is not inserted upon refolding, resulting in its destabilization. The noninserted β-strand may also cause oligomerization of the γ-module. To test these suggestions, we expressed and analyzed truncated variants of the γ-module.

Expression and Characterization of the Truncated Variants of the γ-Module. The recombinant variants of the γ-module expressed for this study are presented in Figure 1C. They include γ-t392 lacking the extreme COOH-terminal residues γ393−411; γ-t373 lacking additional residues, including the β-strand insert (residues γ381−390); and γ-t286 consisting of the NH_2-terminal and the central domain without the β-strand insert. All recombinant fragments formed inclusion bodies in *E. coli*. They were dissolved in 4 M GdmCl, transferred to 8 M urea, and refolded by slow dialysis against 20 mM Tris buffer (pH 8.0), using a protocol elaborated for the preparation of the wild-type recombinant γ-module (*4*) (see Experimental Procedures). The refolded proteins were analyzed by size-exclusion chromatography on Superdex 75. Like γ-wt, the majority of γ-t392 was recovered in the oligomeric form, and only about 15% was eluted as a monomer (Figure 5A). At the same time, the majority of γ-t373 and γ-t286 was recovered in the monomeric form (Figure 5B). The monomeric forms of all four fragments exhibited fluorescence spectra with maxima at 344 nm in comparison with maxima at 352 nm in 4 M GdmCl before slow dialysis (insets in panels A and B of Figure 5); the oligomeric forms of both γ-wt and γ-t392 also exhibited fluorescence spectra with maxima at 344 nm (inset in Figure 5A). These results indicate directly that the oligomerization of γ-wt and γ-t392 upon refolding is connected with the presence of the β-strand insert. They also suggest that all fragments were folded into a compact structure, regardless of their oligomeric state.

The presence of a compact structure in all truncated variants was confirmed in chemical- and heat-induced denaturation experiments. When the truncated γ-t392 variant was titrated with GdmCl while monitoring the ratio of fluorescence intensity at 370 nm to that at 330 nm as a measure of the spectral shift that accompanies unfolding, it exhibited a prominent sigmoidal transition in a denaturant concentration range between 2 and 5 M that was the same as in the wild-type γ-module (compare curves 1 and 2 in Figure 6). This indicates that γ-t392 is folded into a compact structure and that the extreme COOH-terminal residues γ393−411 that are missing in this variant do not contribute to the structural integrity of the γ-module, in agreement with the fact that this region was not well-defined by X-ray (*8*, *9*). The unfolding of the other truncated variant, γ-t373, lacking the extreme COOH-terminal residues and the β-strand insert also occurred in a sigmoidal manner with a similar amplitude, although at lower GdmCl concentrations (Figure 6, curve 3), indicating that without the β-strand insert it is still folded but destabilized. A similar transition was observed in the γ-t286 variant that in addition lacks the COOH-terminal domain (curve 4). The same pattern of relative stability was also observed in the heat-induced denaturation experiments (Figure 7). When heated in the fluorometer while the fluorescence intensity at 370 nm was being monitored, the truncated variant γ-t392 exhibited a prominent sigmoidal transition with a T_m at ∼52 °C that was the same as in the

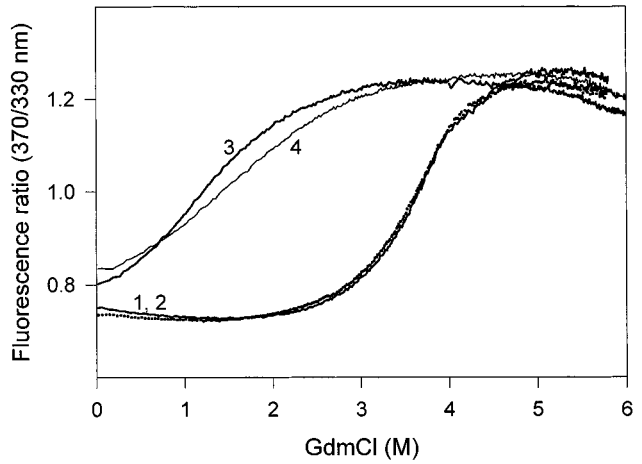

FIGURE 6: Fluorescence-detected denaturation of the recombinant monomeric forms of the γ-module and its truncated variants upon titration with GdmCl. Dotted curve 1 corresponds to the wild-type γ-module; solid curves 2−4 correspond to its truncated variants, γ-t392, γ-t373, and γ-t286, respectively. The curves for the γ-module and γ-t392 essentially coincide. All experiments were performed in 100 mM Gly (pH 8.6) with 0.5 mM Ca^{2+}.

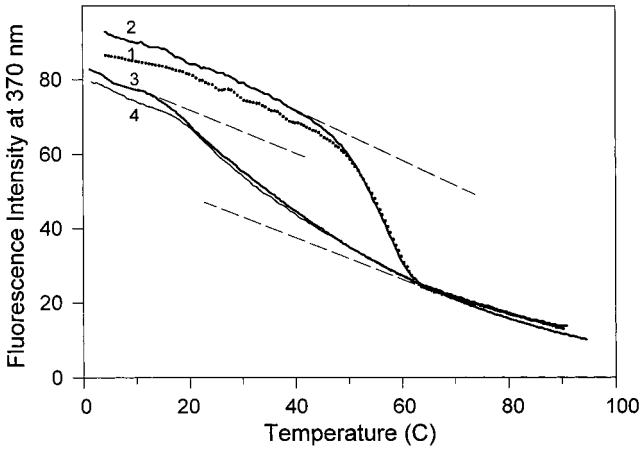

FIGURE 7: Fluorescence-detected thermal denaturation of the recombinant monomeric forms of the γ-module and its truncated variants. Dotted curve 1 corresponds to the wild-type γ-module; solid curves 2−4 correspond to its truncated variants, γ-t392, γ-t373, and γ-t286, respectively. All experiments were performed in 100 mM Gly (pH 8.6) with 0.5 mM Ca^{2+}.

wild-type γ-module[4] (Figure 7, curves 1 and 2). Although the sigmoidal character of the transitions in the other two variants, γ-t373 and γ-t286, was less pronounced (Figure 7, curves 3 and 4), it is still apparent that the unfolding occurred at lower temperatures than that in γ-wt and γ-t392, indicating that their structure is destabilized. All these results indicate that although the β-strand insert is important for the stabilization of the central domain in the γ-module, it may be removed without the loss of the compact structure by the latter.

DISCUSSION

Fibrinogen is rather inert in circulation, but it becomes reactive toward a number of proteins and cell types upon conversion into fibrin or upon binding to some surfaces. Such reactivity, which allows participation of fibrin(ogen) in different physiologically important processes, is often connected with conformational changes that result in the exposure of various interaction sites. Although such changes are well-documented, their molecular basis remains unclear. The availability of the high-resolution structure of the fibrinogen D fragment made it possible to address this question. Here we focus on the mechanism of the function-related conformational changes in its γ-module.

The most striking feature of the γ-module is the unusual β-strand insert in the five-stranded antiparallel β-sheet of its central domain. This feature is reminiscent of a situation reported for the cleaved form of serine protease inhibitors (serpins). Namely, in serpins the cleaved reactive center loop is incorporated as a sixth strand in the center of a previously five-stranded β-sheet (*29*). This insertion, crucial for the inhibitory function of serpins, dramatically increases their thermal stability (*30*−*32*). A similar stabilizing effect can also be achieved by the insertion of synthetic peptides homologous to the reactive center loop (*33*). Serpins are known to polymerize spontaneously upon mild treatment with heat or chemical denaturants (*34*, *35*) or to form polymers upon refolding from inclusion bodies.[5] The mechanism of such polymerization involves the interaction of the reactive center loop of one molecule with the β-sheet(s) of another molecule (*36*, *37*). We kept in mind all these facts about serpins while designing experiments to clarify the role of the β-strand insert in the fibrinogen γ-module.

We first established that the γ374−405 peptide that contains the β-strand region is an integral part of the structure of the D_3 fragment. It should be noted that although D_3 was described long ago and used in numerous studies, this peptide was not previously detected. Then we found that, as in serpins, the removal of this peptide from D_3 destabilized but did not destroy its structure while the addition of the peptide upon refolding of this fragment restored its stability. These results suggested that although the β-strand insert is important for the overall stability of the γ-module, its absence does not prevent refolding. This was confirmed directly with truncated variants of the γ-module; deletion of the β-strand insert resulted in destabilization but did not prevent folding. We also demonstrated that the β-strand insert is required for the formation of oligomers upon refolding of the γ-module since its absence in the truncated γ-t373 and γ-t286 variants prevented formation of such oligomers.

The data presented above indicate that the structural parallel between the β-strand insertion in the γ-module and reactive center loop insertion in serpins results in some similarity between the properties of these proteins. Namely, the reactive center loop and the β-strand insert can cause oligomerization of serpins and the γ-module, respectively, and their removal results in destabilization of both species. On the basis of these similarities together with the established functional reactivity of the COOH-terminal region of the γ-module, one can hypothesize that its β-strand insert may also be functionally important, as in serpins, and that the expression of at least some of its functions could be carried out in a similar manner, namely, by the insertion-removal

[4] We found previously (*4*) that the heat-induced sigmoidal transition in the wild-type γ-module is much better expressed when the unfolding was monitored by the fluorescence intensity at 370 nm instead of the fluorescence ratio.

[5] D. Lawrence, personal communication.

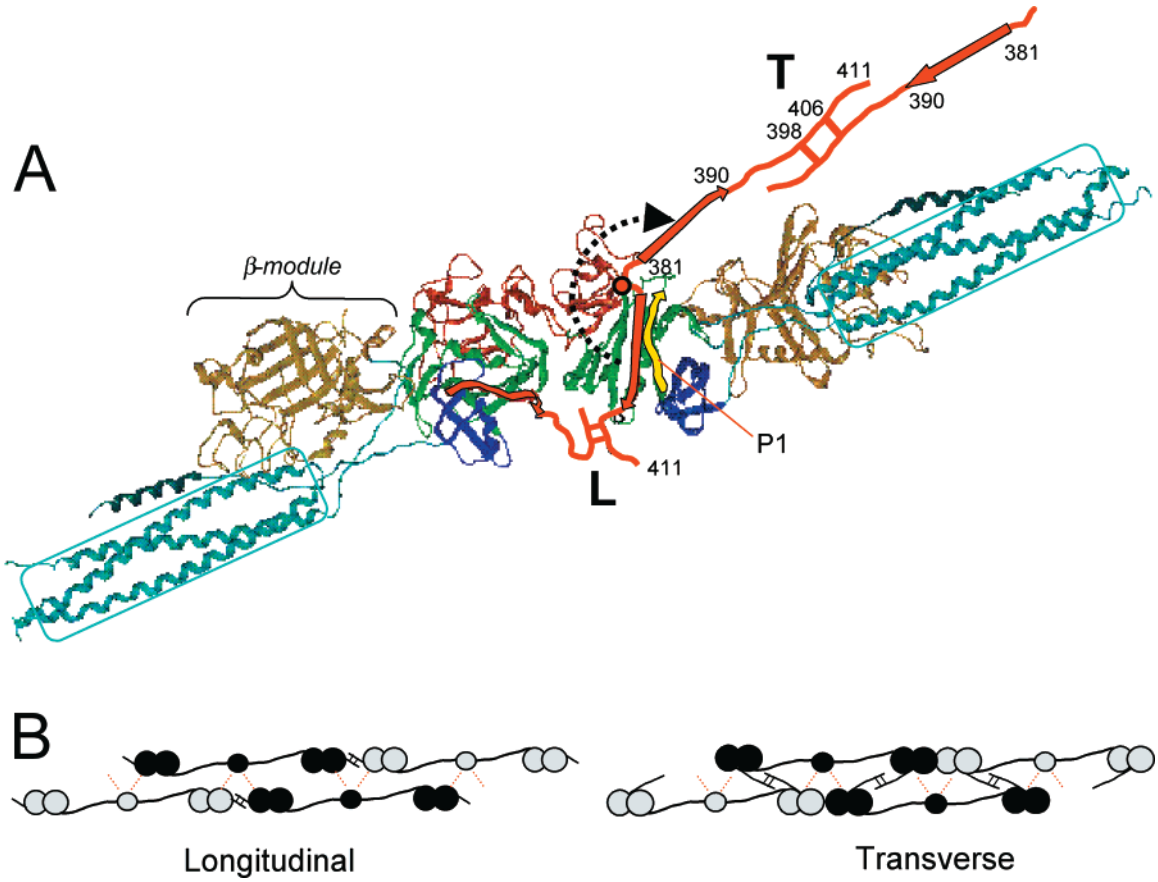

FIGURE 8: Schematic representation of the pull out hypothesis and its application. Panel A represents the ribbon diagram of the dimeric D−D fragment based upon its crystal structure (*9*). The coiled coil domains are boxed; the β-modules are in yellow, and the individual domains in the γ-modules are in blue, green, and yellow as in Figure 1. The γ381−390 β-strand insert in the central domain of each γ-module is presented by a red curved arrow. An antiparallel yellow arrow represents the P1 portion of the Mac-1 binding site (see the text). The extreme COOH-termini of each γ-module (residues 392−411) involved in a longitudinal end-to-end cross-link (L) are represented by red lines linked with two red bars. The curved black dotted arrow shows how the β-strand insert could be pulled out from the central domain to form a transverse cross-link (T). Panel B shows schematically longitudinal and transverse cross-linking in two-stranded protofibril [adopted from Mosesson et al. (*44*)].

(or "pull out") mechanism. We envision that in fibrinogen the β-strand insert could be pulled out of the central domain of the γ-module without destroying the compact structure of the latter (Figure 8A). This would allow the extreme COOH-terminal portion of the γ-chain (γ393−411), which is involved in γ−γ cross-linking and in interaction with some proteins, to be extended from the molecule.

This hypothesis has an immediate application. There is ongoing controversy with respect to whether the factor XIIIa-catalyzed cross-links between fibrin γ-chains are longitudinal, i.e., between γ-chains aligned end-to-end in the same protofibril strand (*9*, *38*−*40*), or transverse, between γ-chains of two adjacent strands (*41*−*45*) (Figure 8B). Electron microscopic data suggest that both may occur. At the same time, a rough calculation of the distance between the γ-modules in fibrin led to the suggestion that transverse cross-linking is unlikely (*8*). The finding by Spraggon et al. (*9*) that the COOH-terminal regions of two γ-chains in the dimeric D fragment are closely spaced reinforced that concept. Our hypothesis allows us to reconcile the basis for formation of transverse γ−γ cross-links. Namely, if the β-strand insert is pulled out of the γ-module, each COOH-terminus containing reactive Gln398/399 and Lys406 could easily extend an additional 35 Å, a distance sufficient to form a transverse cross-link (Figure 8A).

It should be stressed that this hypothesis does not rule out the end-to-end cross-links that probably occur between the D domains in the D−D fragment in whose γ-modules the β-strands are inserted. It suggests a mechanism by which the γ-module may change its conformation to create the possibility for transverse γ−γ cross-links. In this respect, the crystal structure of the D−D fragment that revealed that the COOH-terminal regions of two neighboring γ-chains are in proximity (*9*) may reflect only one of the possible conformations that the γ-module can adopt. In agreement, Mosesson et al. (*45*) demonstrated by electron microscopy that the Au_{11}-cadaverine-labeled Gln398 and -399 residues in fibrinogen could be observed in different positions relative to the extreme end of the molecule. The appearance of some of them as far away as 8−12 nm from the end would require the removal of the β-strand insert to extend the COOH-terminus that much (Figure 8A). This is in good agreement with our hypothesis and reinforces it.

The pull out mechanism could be involved in regulation of fibrinogen−leukocyte interactions during an inflammatory response. Indeed, the β-strand insert (γ381−390) represents part of the leukocyte-binding site that provides interaction with leukocyte receptor Mac-1 (*18*). This site is composed of two sequences, γ190−202 (P1) and γ377−395 (P2) (Figures 1 and 8), that form adjacent antiparallel β-strands

(*16*, *18*). Obviously, the pull out of one of these strands (P2) should affect this interaction. Interestingly, synthetic peptides mimicking the P1 and P2 sequences both support leukocyte adhesion when immobilized to a surface (*18*). This suggests that P1 and P2 may act independently in fibrin(ogen) after removal of the β-strand inserts from the γ-modules. The natural and recombinant fragments described in this study may represent useful tools for further clarification of the role of the β-strand insert in fibrin(ogen)−leukocyte interaction.

The pull out mechanism could also be involved in the exposure of the receptor-induced binding site (RIBS-1) localized to the γ373−385 region of fibrinogen (*20*, *21*). This site is recognized by a specific monoclonal antibody only when platelet receptor $\alpha_{IIb}\beta_3$ binds to the γ400−411 region of fibrinogen (*21*). One can speculate that the anchoring of fibrinogen to platelets via this region may facilitate the removal of the β-strand insert (γ381−390) from the central domain of the γ-module. This, in turn, should change the conformation of the γ373−385 region that may result in the exposure of RIBS-1. Although the nature of the forces that would pull out the insert remains to be established, the above speculation may provide a useful hint for the search for such forces.

The crystal structure of two other fibrinogen modules from the β-chain and an extended version of the Aα-chain, both homologous to the γ-module, revealed that they are folded like the γ-module (*9*, *46*), suggesting that their β-strand inserts may also play a role in their conformational mobility. However, these modules, as well as a number of other homologous fibrinogen-related modules found in various proteins, do not contain the extreme COOH-terminal extension present in the γ-module (*8*, *47*). Thus, if "anchoring" via this region is indeed important for the removal of the insert as speculated above, the pull out mechanism may not be applicable to these modules. On the other hand, such extension is not unique for the γ-module; a COOH-terminal extension is also found in the fibrinogen-related modules of several tenascins (*8*). Although it is not homologous to that of the γ-module, it contains a cluster of basic amino acid residues which may be responsible for binding of this module to heparin (*48*) and could anchor tenascins to cell-surface proteoglycans.

In summary, we demonstrated in this study that the β-strand insert can be removed from the central domain of the γ-module without the loss of the compact fold of the latter. On the basis of this and some other observations, we proposed a pull out hypothesis that allows us to explain transverse $\gamma-\gamma$ cross-linking in fibrin and to clarify the mechanism of exposure of some function-related binding sites.

ACKNOWLEDGMENT

We thank Dr. K. Ingham, Dr. M. Mosesson, and Dr. D. Lawrence for helpful criticism during preparation of the manuscript.

REFERENCES

1. Doolittle, R. F. (1984) *Annu. Rev. Biochem. 53*, 195−229.
2. Privalov, P. L., and Medved, L. V. (1982) *J. Mol. Biol. 159*, 665−683.
3. Medved, L. V., Gorkun, O. V., and Privalov, P. L. (1983) *FEBS Lett. 160*, 291−295.
4. Medved, L., Litvinovich, S., Ugarova, T., Matsuka, Y., and Ingham, K. (1997) *Biochemistry 36*, 4685−4693.
5. Nieuwenhuizen, W., Vermond, A., Voskuilen, M., Traas, D. W., and Verheijen, J. H. (1983) *Biochim. Biophys. Acta 748*, 86−92.
6. Bosma, P. J., Rijken, D. C., and Nieuwenhuizen, W. (1988) *Eur. J. Biochem. 172*, 399−404.
7. Altieri, D. C. (1999) *Thromb. Haemostasis 82*, 781−786.
8. Yee, V. C., Pratt, K. P., Cote, H. C. F., Le Trong, I., Chung, D. W., Davie, E. W., Stenkamp, R. E., and Teller, D. C. (1997) *Structure 5*, 125−138.
9. Spraggon, G., Everse, S. J., and Doolittle, R. F. (1997) *Nature 389*, 455−462.
10. Everse, S. J., Spraggon, G., Veerapandian, L., Riley, M., and Doolittle, R. F. (1998) *Biochemistry 37*, 8637−8642.
11. Shimizu, A., Nagel, G. M., and Doolitle, R. F. (1992) *Proc. Natl. Acad. Sci. U.S.A. 89*, 2888−2892.
12. Pratt, K. P., Cote, H. C., Chung, D. W., Stenkamp, R. E., and Davie, E. W. (1997) *Proc. Natl. Acad. Sci. U.S.A. 94*, 7176−7181.
13. Chen, R., and Doolittle, R. F. (1971) *Biochemistry 10*, 4486−4491.
14. Yonekawa, O., Voskuilen, M., and Nieuwenhuizen, W. (1992) *Biochem. J. 283*, 187−191.
15. Niewiarowski, S., Kornecki, E., Budzynski, A. Z., Morinelli, T. A., and Tuszynski, G. P. (1983) *Ann. N.Y. Acad. Sci. 408*, 536−555.
16. Altieri, D. C., Plescia, J., and Plow, E. F. (1993) *J. Biol. Chem. 268*, 1847−1853.
17. Hawiger, J., Kloczewiak, M., Timmons, S., Strong, D., and Doolittle, R. F. (1983) *Ann. N.Y. Acad. Sci. 408*, 521−535.
18. Ugarova, T. P., Solovjov, D. A., Zhang, L., Loukinov, D. I., Yee, V. C., Medved, L. V., and Plow, E. F. (1998) *J. Biol. Chem. 273*, 22519−22527.
19. Solovjov, D. A., Kudryk, B., Plow, E. F., and Ugarova, T. P. (1999) *Blood 94* (Suppl. 1), 428a.
20. Zamarron, C., Ginsberg, M. H., and Plow, E. F. (1990) *Thromb. Haemostasis 64*, 41−46.
21. Zamarron, C., Ginsberg, M. H., and Plow, E. F. (1991) *J. Biol. Chem. 266*, 16193−16199.
22. Cierniewski, C. S., Kloczewiak, M., and Budzynski, A. Z. (1986) *J. Biol. Chem. 261*, 9116−9121.
23. Nieuwenhuizen, W., Voskuilen, M., Vermond, A., Haverkate, F., and Hermans, J. (1982) *Biochim. Biophys. Acta 707*, 190−192.
24. Gill, S. C., and von Hippel, P. H. (1989) *Anal. Biochem. 182*, 319−326.
25. Edelhoch, H. (1967) *Biochemistry 6*, 1948−1954.
26. Privalov, P. L., and Potekhin, S. A. (1986) *Methods Enzymol. 131*, 4−51.
27. Filimonov, V. V., Potekhin, S. A., Matveev, S. V., and Privalov, P. L. (1982) *Mol. Biol. (Moscow) 16*, 551−562.
28. Haverkate, F., and Timan, G. (1977) *Thromb. Res. 10*, 803−812.
29. Loebermann, H., Tokuoka, R., Deisenhofer, J., and Huber, R. (1984) *J. Mol. Biol. 177*, 531−557.
30. Carrell, R. W., and Owen, M. C. (1985) *Nature 317*, 730−732.
31. Bruch, M., Weiss, V., and Engel, J. (1988) *J. Biol. Chem. 263*, 16626−16630.
32. Lawrence, D. A., Olson, S. T., Palaniappan, S., and Ginsburg, D. (1994) *J. Biol. Chem. 269*, 27657−27662.
33. Lawrence, D. A. (1997) *Adv. Exp. Med. Biol. 425*, 99−108.
34. Mikus, P., Urano, T., Liljestrom, P., and Ny, T. (1993) *Eur. J. Biochem. 218*, 1071−1082.
35. Lomas, D. A., Elliott, P. R., Sidhar, S. K., Foreman, R. C., Finch, J. T., Cox, D. W., Whisstock, J. C., and Carrell, R. W. (1995) *J. Biol. Chem. 270*, 16864−16870.

36. Chang, W. S., Whisstock, J., Hopkins, P. C., Lesk, A. M., Carrell, R. W., and Wardell, M. R. (1997) *Protein Sci. 6*, 89−98.
37. Dunstone, M. A., Dai, W., Whisstock, J. C., Rossjohn, J., Pike, R. N., Feil, S. C., Le Bonniec, B. F., Parker, M. W., and Bottomley, S. P. (2000) *Protein Sci. 9*, 417−420.
38. Fowler, W. E., Erickson, H. P., Hantgan, R. R., McDonagh, J., and Hermans, J. (1981) *Science 211*, 287−289.
39. Weisel, J. W., Francis, C. W., Nagaswami, C., and Marder, V. J. (1993) *J. Biol. Chem. 268*, 26618−26624.
40. Veklich, Y., Ang, E. K., Lorand, L., and Weisel, J. W. (1998) *Proc. Natl. Acad. Sci. U.S.A. 95*, 1438−1442.
41. Selmayr, E., Thiel, W., and Muller-Berghaus, G. (1985) *Thromb. Res. 39*, 459−465.
42. Mosesson, M. W., Siebenlist, K. R., Amrani, D. L., and DiOrio, J. P. (1989) *Proc. Natl. Acad. Sci. U.S.A. 86*, 1113−1117.
43. Siebenlist, K. R., Meh, D. A., Wall, J. S., Hainfeld, J. F., and Mosesson, M. W. (1995) *Thromb. Haemostasis 74*, 1113−1119.
44. Mosesson, M. W., Siebenlist, K. R., Hainfeld, J. F., and Wall, J. S. (1995) *J. Struct. Biol. 115*, 88−101.
45. Mosesson, M. W., Siebenlist, K. R., Meh, D. A., Wall, J. S., and Hainfeld, J. F. (1998) *Proc. Natl. Acad. Sci. U.S.A. 95*, 10511−10516.
46. Spraggon, G., Applegate, D., Everse, S. J., Zhang, J. Z., Veerapandian, L., Redman, C., Doolittle, R. F., and Grieninger, G. (1998) *Proc. Natl. Acad. Sci. U.S.A. 95*, 9099−9104.
47. Doolittle, R. F. (1992) *Protein Sci. 1*, 1563−1577.
48. Fischer, D., Chiquet-Ehrismann, R., Bernasconi, C., and Chiquet, M. (1995) *J. Biol. Chem. 270*, 3378−3384.

BI001836H